

Neurons arise in the basal neuroepithelium of the early mammalian telencephalon: A major site of neurogenesis

Wulf Haubensak*, Alessio Attardo*, Winfried Denk†, and Wieland B. Huttner**

*Max Planck Institute of Molecular Cell Biology and Genetics, Pfotenhauerstrasse 108, D-01307 Dresden, Germany; and †Max Planck Institute for Medical Research, Jahnstrasse 29, D-69120 Heidelberg, Germany

Communicated by Kai Simons, Max Planck Institute of Molecular Cell Biology and Genetics, Dresden, Germany, December 23, 2003 (received for review December 15, 2003)

Neurons of the mammalian CNS are thought to originate from progenitors dividing at the apical surface of the neuroepithelium. Here we use mouse embryos expressing GFP from the *Tis21* locus, a gene expressed throughout the neural tube in most, if not all, neuron-generating progenitors, to specifically reveal the cell divisions that produce CNS neurons. In addition to the apical, asymmetric divisions of neuroepithelial (NE) cells that generate another NE cell and a neuron, we find, from the onset of neurogenesis, a second population of progenitors that divide in the basal region of the neuroepithelium and generate two neurons. Basal progenitors are most frequent in the telencephalon, where they outnumber the apically dividing neuron-generating NE cells. Our observations reconcile previous data on the origin and lineage of CNS neurons and show that basal, rather than apical, progenitors are the major source of the neurons of the mammalian neocortex.

All neurons generated during the development of the mammalian CNS derive from neuroepithelial (NE) cells (see *Supporting Text*, which is published as supporting information on the PNAS web site). NE cells undergo three principal kinds of cell division, (i) symmetric, proliferative divisions (two NE cells) (see *Supporting Text* for terminology), (ii) asymmetric divisions (one NE cell, one neuron) and (iii) symmetric, differentiating divisions (two neurons) (1–6). It remains to be settled whether, at the very onset of neurogenesis, NE cells switch only to asymmetric division, or to both asymmetric and symmetric differentiating divisions.

Real-time imaging studies of cells dividing at the apical surface of the neuroepithelium (7–9) and analyses of intrinsic cell fate determinants with a polarized distribution in mitotic NE cells (7, 10, 11) have provided evidence in support of the widely held view that during early neurogenesis, neurons are generated from NE cells by asymmetric rather than symmetric differentiating divisions (2, 6, 12–14). In contrast, consistent with retroviral lineage tracing studies *in vivo* (5, 15–18), analysis of the division patterns of isolated NE cells and their progeny has documented the coexistence, *in vitro*, of asymmetric and symmetric neuron-generating divisions of progenitors at the onset of neurogenesis (19–21). One possible explanation for this apparent discrepancy is the existence of neuronal progenitors other than the canonical NE cell dividing at the apical surface of the neuroepithelium.

One of the problems in studying the divisions of NE cells that generate neurons has been the lack of a marker that allows one to distinguish between proliferating and neuron-generating NE cells and to identify the latter before they enter mitosis. Our group previously reported the first such marker, *Tis21*, an antiproliferative gene that within the neural tube is selectively expressed in neuron-generating, but not proliferating, NE cells, nor in neurons (22). Moreover, given that >95% of the newborn CNS neurons appear to inherit TIS21 protein from their progenitors (22), *Tis21* is presumably expressed in the vast majority, if not all, of neuronal progenitors, an important aspect in view of the possible existence of as yet uncharacterized subpopulations of such cells. Here, we have generated a *Tis21*-GFP

knock-in mouse line and, by using time-lapse multiphoton microscopy, we have analyzed neuron-generating divisions in the embryonic neural tube at the onset of neurogenesis.

Methods

Generation of *Tis21*-GFP Knock-In Mice. For details about the generation of *Tis21*-GFP knock-in mice ($Tis21^{+/tm2(Gfp)Wbh}$), see *Supporting Text*. All data shown in this study are from heterozygous embryos obtained by crossing homozygous males to C57BL/6J females. The day of the vaginal plug was defined as embryonic day (E) 0.5.

Fluorescence Microscopy on Whole-Mounts and Cryosections. Fluorescence microscopy on whole-mounts and cryosections was performed according to standard procedures. Details are given in *Supporting Text*.

Definitions and Quantitations. “Apical mitoses” were defined as those occurring at the apical (ventricular) surface of the neuroepithelium. “Subapical mitoses” were defined as nonsurface mitoses that were at most three nuclear diameters away from the apical surface of the neuroepithelium. “Basal mitoses” were defined as those occurring in the basal one-third of the ventricular zone (VZ), which is referred to as its “basal portion” or “basal region.”

The abundance of GFP-containing cells in the VZ (Fig. 1j) was determined by counting the nuclei showing GFP fluorescence and expressing these as percentage of 4',6-diamidino-2-phenylindole (DAPI)-stained nuclei. For the quantitation of mitotic cells in the VZ and (when present) subventricular zone (SVZ) (Fig. 2j–m), mitotic cells were identified by phosphohistone H3 staining, corroborated by DAPI staining, and the proportion of mitotic cells showing GFP fluorescence was determined. Basal mitotic GFP-positive cells were also analyzed for β III-tubulin immunoreactivity.

Multiphoton Time-Lapse Video Microscopy. Brain slices (250–400 μ m) from E9.5–E12.5 heterozygous *Tis21*-GFP knock-in mouse embryos were prepared following established methods (23) and cultured in a POC-Chamber system (Saur, Reutlingen, Germany) in Neurobasal medium (Invitrogen) supplemented with 10% immediately centrifuged mouse serum (Harlan Breeding Laboratories), 1 \times N2 (Invitrogen), 1 \times B27 supplement (Invitrogen) and 100 units/ml penicillin/streptomycin. The POC-Chamber system was gassed with 20% O₂/5% CO₂/75% N₂. For details, see *Supporting Text*.

Time-lapse analysis was usually started \approx 2 h after the beginning of the culture, after visual verification of the integrity of the slice.

Abbreviations: NE, neuroepithelial; En, embryonic day *n*; VZ, ventricular zone; SVZ, subventricular zone.

†To whom correspondence should be addressed. E-mail: huttner@mpi-cbg.de.

© 2004 by The National Academy of Sciences of the USA

Images were recorded on an inverted Radiance 2100 multiphoton microscope (Bio-Rad) equipped with Nikon optics (ECLIPSE TE300) and a Mira 900 titanium/sapphire laser (Coherent) tuned to 900 nm, which was pumped by a Verdi 5 W solid-state laser (Coherent). A $\times 60$ water immersion lens, which was heated to 37°C by using an objective heater (Bioptechs) and constantly supplied with immersion water by using a pump, was used to record the GFP fluorescence. Every 5–10 min, 100- μm z stacks, with the individual optical sections being spaced at 3- or 5- μm intervals, were recorded by using a single scanning run at 256 \times 256 pixel resolution with a scanning speed of 133–500 lines per second. Images were acquired by using the Bio-Rad software. Three-dimensional reconstructions were computed by using VOLOCITY software (Improvision) in either the high-resolution (HR) rendering or 3D-rendering mode (see figure legends).

The amount of GFP fluorescence and nuclear size were quantified from the raw data (Bio-Rad) by using NIH 1.62 software (National Institutes of Health). For details, see *Supporting Text*.

Results

A *Tis21*-GFP Knock-In Mouse Reveals Neuron-Generating Progenitors in the Embryonic CNS. We first established a *Tis21*-GFP knock-in mouse line in which the protein-encoding portion of exon 1 of the *Tis21* gene was replaced by GFP carrying a nuclear localization signal (see Fig. 5, which is published as supporting information on the PNAS web site). The appearance of GFP fluorescence in the developing CNS of E9.5–E14.5 heterozygous *Tis21*-GFP knock-in mouse embryos (Fig. 1 *a–d*) completely matched the known expression of *Tis21* mRNA (22, 24) and correlated precisely with the temporal and spatial gradients of neurogenesis. This was corroborated by analysis of GFP fluorescence (the pattern of which was essentially identical to that of GFP immunoreactivity; data not shown) and β III-tubulin immunoreactivity, a marker of young neurons (25), in sections of the developing CNS. We studied the gradients of neurogenesis by examining, at a magnification allowing an overview of the neural tube wall, either one defined brain region (telencephalon) over time (E9.5–E15.5) (Fig. 1 *e–j*) or various regions of the CNS along the rostro-caudal axis (telencephalon–spinal cord) at one defined developmental time point (E10.5) (see Fig. 6, which is published as supporting information on the PNAS web site), with essentially the same principal results.

No *Tis21*-driven GFP expression was detected in the neuroepithelium before the onset of neurogenesis (Fig. 1*e*). At the onset of neurogenesis (Fig. 1*f*), a few cells in the VZ (Fig. 1*j*, E10.5), which lacked β III-tubulin immunoreactivity and were therefore NE cells, started to express GFP. The fluorescence was confined to the nucleus, as expected from the presence of a nuclear localization signal. Consistent with the notion that *Tis21*-expressing NE cells generate neurons (22), virtually all of the newborn neurons (as identified by the presence of β III-tubulin immunoreactivity) in the VZ (Fig. 2*h*, arrowhead), and still most of the slightly older neurons (“young neurons”) in the adjacent neuron-containing layer (Fig. 1*f*, asterisk, and Fig. 2*d*, solid white arrowhead), showed GFP fluorescence (see Table 1, which is published as supporting information on the PNAS web site). Newborn and young neurons are known to lack *Tis21* gene expression (22). The presence of GFP fluorescence in these neurons therefore reflected the inheritance, by default, of the GFP protein from NE progenitors exhibiting *Tis21*-driven GFP expression (see Fig. 4*e*). This, in turn, implies that most, if not all, neurons are derived from *Tis21*-GFP-expressing progenitors.

Concomitant with the progress in neurogenesis, the proportion of GFP-expressing NE cells increased (Fig. 1 *f–i*), with 60% of all cells of the E15.5 telencephalic VZ expressing GFP (Fig. 1*j*). The GFP-positive nuclei appeared to be more abundant and to show brighter fluorescence in the basal than in the apical portion of the VZ. This reflects the fact that (i) the *Tis21* gene is transiently

expressed in the G₁-phase of the cell cycle (22) and, hence, GFP fluorescence peaks when neuron-generating progenitors are in S phase, and (ii) the nuclei of a substantial portion of the neuron-generating progenitors do not migrate to the apical surface in G₂ but remain in the basal region of the VZ, as will be described below. At these later stages of neurogenesis, only few cells in the neuronal layers still showed GFP fluorescence, and there was a clear apical-to-basal decline in both frequency and intensity of these cells (Fig. 1, compare *h* and *i*).

Based on the findings that (i) the onset and progression of *Tis21*-driven GFP expression in NE cells correlates precisely with the onset and progression of neurogenesis and (ii) most, if not all, neurons are derived from *Tis21*-GFP-expressing progenitors, and in view of the time-lapse observations described below, we conclude that, during early neurogenesis in *Tis21*-GFP knock-in mouse embryos, divisions of *Tis21*-GFP-expressing cells in the neuroepithelium generate neurons.

A Mitotic Neuron-Generating Progenitor at the Basal Side of the VZ.

We therefore focused on the mitotic cells in the neuroepithelium showing *Tis21*-driven GFP expression. In the E10.5 hindbrain, consistent with some interphase NE cells expressing GFP (Fig. 2*h*, arrow), some of the mitotic cells at the apical surface of the neuroepithelium showed GFP fluorescence (Fig. 2 *e–g*, open arrows). More apical mitotic cells became GFP-positive as neurogenesis progressed (Fig. 2*m*, curve A).

Surprisingly, however, even at the onset of neurogenesis, GFP-positive mitotic cells were observed not only at the apical surface of the neuroepithelium, but also in the basal region of the VZ, as illustrated for the E10.5 telencephalon (Fig. 2 *a–d*, open arrows with asterisk). Like the apical GFP-positive mitotic NE cells, the GFP-positive mitotic cells in the basal portion of the neuroepithelium were undetectable before the onset of neurogenesis. As neurogenesis in the telencephalon progressed, the basal GFP-positive mitotic cells (Fig. 2*l*, curve B) increased more rapidly in number than the apical ones and outnumbered the latter (Fig. 2*l*, curve A). The time course of the sum of apical plus basal GFP-positive mitotic cells (Fig. 2*l*, curve A+B) was consistent with that of the total (mitotic plus interphase) GFP-positive cells in the telencephalic neuroepithelium (Fig. 1*j*). Along the rostro-caudal axis of the neural tube, basal GFP-positive mitotic cells were most frequently observed in the regions that are known to form a SVZ at later stages of neuro- and gliogenesis (26), i.e., the telencephalon (Fig. 2, compare *l* and *m*, curves B). Indeed, the basal GFP-positive mitotic cells were found to be abundant in the SVZ of the E13.5 telencephalon (Fig. 3*i*, filled white arrowheads).

In the telencephalon, almost all ($\approx 90\%$) of the basal mitotic cells observed at the onset of neurogenesis were found to express GFP (Fig. 2*j*, E10.5), and the same was the case once a SVZ had formed (Fig. 2*j*, E13.5). The vast majority ($>90\%$) of the basal mitotic GFP-positive cells did not show β III-tubulin immunoreactivity (Fig. 2*d*, open arrow with asterisk), which was detected in only 2 of 31 cells analyzed.

We conclude that, from the onset of neurogenesis in the mouse embryonic telencephalon, neurogenic progenitors dividing at the basal side of the VZ coexist with those dividing at the apical side, and eventually outnumber the latter.

Apical Neuron-Generating Progenitors Undergo Asymmetric Division.

Next, we studied, during early stages of neurogenesis, the behavior of the GFP-expressing cells dividing at the apical and the basal side of the VZ, and also that of the resulting daughter cells (see *Supporting Text* for subapical divisions, and Figs. 7*d* and 8, which are published as supporting information on the PNAS web site). For this purpose, we used time-lapse multiphoton laser scanning microscopy (27) of organotypic slice cultures of E12.5 telencephalon, an established experimental system (28). In the

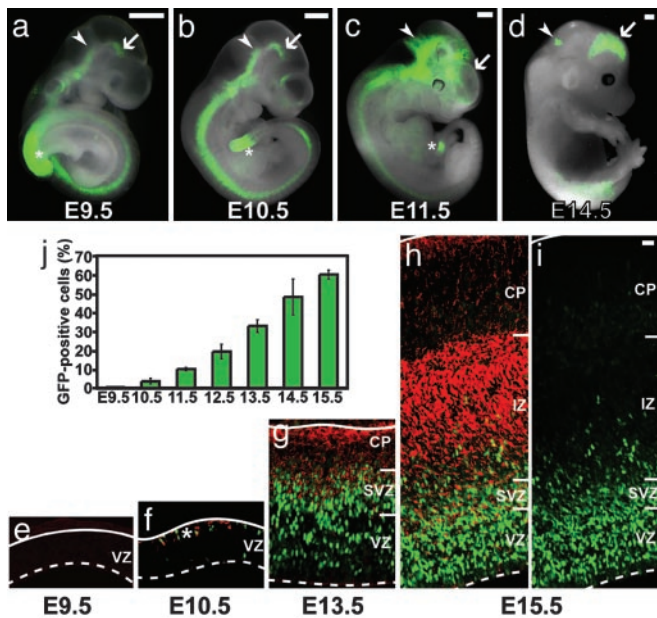


Fig. 1. Heterozygous *Tis21*-GFP knock-in mouse embryos show GFP expression in the developing CNS in temporal and spatial correlation with neurogenesis. (a–d) GFP fluorescence in unfixed whole-mount preparations at various developmental stages. Arrows indicate the ventral midbrain (a and b) or the dorsal telencephalon (c and d); arrowheads the mid-hindbrain boundary (a–c) or the developing cerebellum (d). Note the spreading of GFP expression in the rostral and dorsal directions during development. Asterisks indicate the tailbud. (Scale bars, 500 μ m.) (e–i) GFP fluorescence (green) and β III-tubulin immunoreactivity (red) in cryosections of dorsal telencephalon at various developmental stages; *i* is the same cryosection as *h* except that the signal for β III-tubulin immunoreactivity was omitted to facilitate the observation of GFP fluorescence in the neuronal layers. Solid white lines, basal lamina; dashed white lines, apical surface of neuroepithelium. IZ, intermediate zone, CP, cortical plate; NL, neuronal layers; asterisk in *f*, layer of the first neurons at the basal side of the VZ. (e–i are the same magnification; scale bar in the top right corner of *i*, 20 μ m.) (j) Time course of the appearance of GFP-positive cells in the telencephalic VZ during embryonic neurogenesis, expressed as percentage of total VZ cells. Data are the mean of two embryos (>200 total cells counted per time point and embryo); bars indicate the variation of the individual values from the mean.

case of the apically dividing cells, the GFP-labeled nucleus of the mother cell migrated from the basal to the apical side of the neuroepithelium, followed by cell division and migration of the daughter cell nuclei in the basal direction (Figs. 3a and 7 a–c, and Movie 1 and Table 2, which are published as supporting information on the PNAS web site). In virtually all cases, the daughter cells behaved differently from each other in several respects.

First, the basally directed migration of the daughter cell nuclei was distinct, with one nucleus (referred to as the leading nucleus, Fig. 3a arrowheads) moving ahead of the other (referred to as the trailing nucleus, Fig. 3a arrows; see also Fig. 9, which is published as supporting information on the PNAS web site). Second, the destination of the daughter cells originating from apical divisions differed. Whenever the leading nucleus could be followed for a sufficiently long time, it left the VZ (Fig. 3a, 380 min arrowhead) and apparently entered the adjacent layer containing young neurons (Fig. 7 a–c arrowheads). In contrast, the trailing nucleus eventually returned to the apical surface and underwent another mitosis (Fig. 3b arrows). Third, the daughter cells originating from apical divisions were different with regard to the intensity of GFP fluorescence over time. Relative to the leading daughter cell nucleus, the trailing nucleus consistently showed an at least 2-fold increase in GFP fluorescence within the

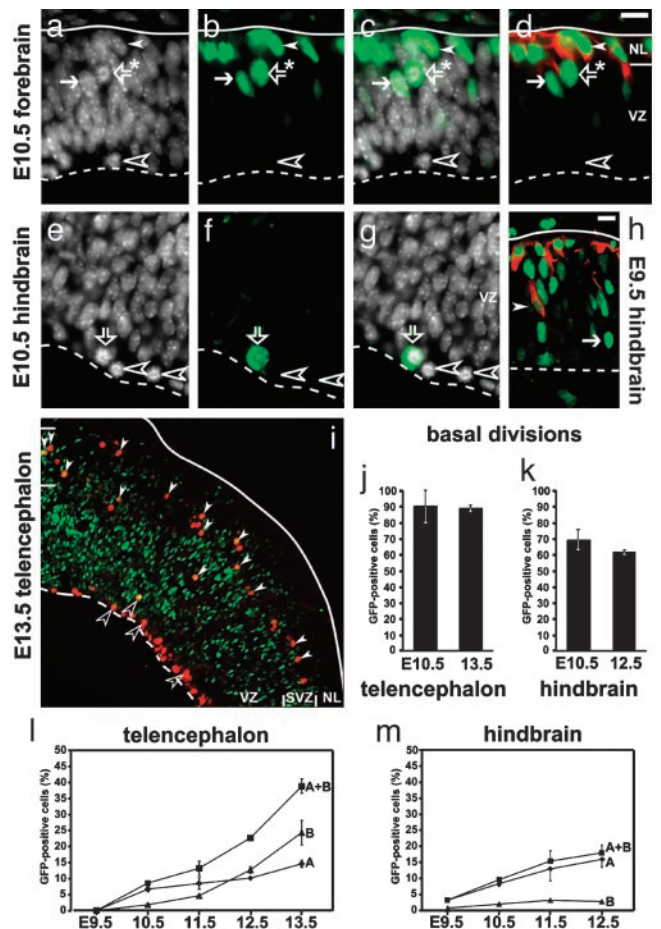


Fig. 2. Not only a subpopulation of the mitotic cells at the apical side of the neuroepithelium, but also mitotic cells in the basal portion of the VZ and in the SVZ, show *Tis21*-driven GFP expression. (a–h) 4',6-Diamidino-2-phenylindole staining (white; a, c, e, and g), GFP fluorescence (Green; b–d and f–h), and β III-tubulin immunofluorescence (red; d and h) of the E10.5 telencephalon (a–d), E10.5 hindbrain (e–g), and E9.5 hindbrain at lower magnification (h). Solid white lines, basal lamina; dashed white lines, apical surface; arrows, GFP-expressing NE cells in interphase; open white arrowheads, mitotic NE cells lacking GFP. (a–d) Scale bar in top right corner of *d*, 20 μ m. (a–d) Note the mitotic cell (open arrows with asterisk) in the basal portion of the VZ, which expresses GFP (b–d) but not β III-tubulin (d), in contrast to the young neurons (solid white arrowheads; NL, neuron-containing layer), which contain both GFP (b–d) and β III-tubulin (d). (e–g) At the apical surface of the VZ, mitotic NE cells lacking GFP are observed (open white arrowheads), which may coexist with mitotic NE cells expressing GFP (open arrows). (h) A newborn neuron (solid white arrowhead) in the VZ. (i) Low-power overview of the E13.5 telencephalon showing mitotic cells, identified by phosphohistone H3 immunostaining (red), at the apical surface (dashed white line) of the VZ and in the SVZ but not in the overlying neuron-containing layer (NL; solid white line, basal lamina). Mitotic cells in the VZ and SVZ showing GFP fluorescence (green) upon individual inspection at higher magnification (not shown) are indicated by open and filled white arrowheads, respectively; note that in the merged image shown, the phosphohistone H3 immunostaining (red) largely obscures the signal for GFP fluorescence, except for mitotic cells with high GFP levels (yellow). (j and k) Quantitation of mitotic GFP-positive cells in the basal portion of the VZ (plus, when present, the SVZ) of the telencephalon at E10.5 and E13.5 (j) and hindbrain at E10.5 and E12.5 (k), expressed as percentage of total mitotic cells in the basal portion of the VZ (plus, when present, the SVZ) (4–140 cells counted per embryo). (l and m) Quantitation of mitotic GFP-positive cells at the apical side of the neuroepithelium (A, diamonds) and in the basal portion of the VZ (plus, when present, the SVZ) (B, triangles), each expressed as percentage of total mitotic cells at the apical side of the neuroepithelium (130–900 cells counted per embryo), as well as the sum of both (A+B, squares), in the telencephalon (l) and hindbrain (m) at various developmental stages. (j–m) Data are the mean of two embryos (except for E9.5, which is a single embryo); bars indicate the variation of the individual values from the mean and are sometimes included within the symbol.

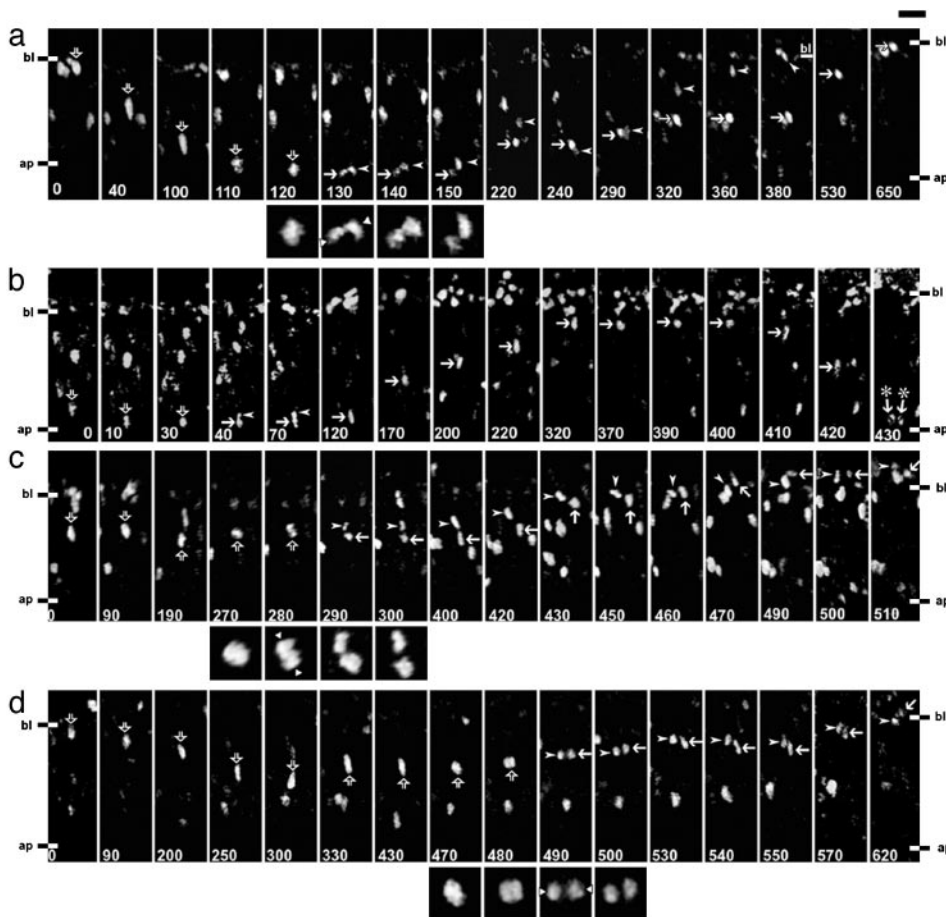


Fig. 3. Time-lapse multiphoton laser scanning microscopy, using slice cultures of E12.5 telencephalon, of cells in the VZ showing *Tis21*-driven GFP expression. Shown are examples of cells dividing at the apical surface (*a* and *b*) or in the basal region (*c* and *d*), and their progeny (HR-rendering mode). (*a–d*) bl, basal boundary of VZ (note that, at later stages of the time-lapse, this boundary shifts upwards in the panels shown due to growth of the VZ); ap, apical surface, which runs horizontally across the bottom of each panel as indicated; open arrows, mother cell; arrowheads and arrows, daughter cells. The time of observation is indicated in min at the bottom of each panel. The square panels underneath *a*, *c*, and *d* show the mitoses at higher magnification and with enhanced fluorescent signal; the two white triangles at the margins indicate the initial position of the daughter cell nuclei (parallel, oblique, or perpendicular to ventricular surface). [Scale bar above top right panel in *a*, 20 μm (rectangular panels) and 10 μm (square panels).] (*a*) The elongated mother cell nucleus migrates toward the apical surface (0–110 min); the cell rounds up for mitosis (110–120 min); the initial position of the daughter cell nuclei is parallel to the ventricular surface (130 min), followed by their rotation (130–150 min); the daughter cell nuclei migrate separately in the basal direction (150–220 min); the leading nucleus then turns around (220 min), migrating apically toward (220–240 min), and then basally together with (240–290 min) the trailing one; and finally separates from the latter to migrate to and beyond the basal boundary of the VZ (290–530 min, note basal boundary at 380 min), followed by the trailing nucleus, which eventually reaches this boundary (290–650 min, note the shift in basal boundary from 380 min to 650 min). (*b*) The mother cell nucleus migrates toward the apical surface (0–10 min); the cell rounds up for mitosis (30 min) and apparently generates an apical and a basal daughter cell, which remain in close proximity to each other (40–70 min) and of which the apical one (arrows) was tracked; the apical daughter cell nucleus migrates to the basal side of the VZ (120–320 min), pauses there (320–400 min), and migrates rapidly back to the apical surface (400–430 min) followed by mitosis (430 min, arrows with asterisks). (*c*) The nucleus of the mother cell pauses in the basal half of the VZ, with subtle basal–apical–basal movement (0–270 min), the cell divides in the basal region of the VZ (270–300 min) with the initial position of the daughter cell nuclei being perpendicular to the ventricular surface (280 min), and both daughter cell nuclei migrate together basally into the adjacent neuronal layer (300–510 min). Note that the long axis of the ellipsoid daughter cell nuclei loses the strict radial orientation, which it shows while migrating in the VZ (arrowheads, 300–420 min; arrows, 300–450 min), upon entering the neuronal layer (arrowheads, 430–460 min; arrows, 470–490 min). (*d*) The nucleus of the mother cell migrates in the apical direction but does not divide (0–300 min), turns around and pauses (300–430 min), the cell divides in the basal region of the VZ (470–500 min) with an initial position of the daughter cell nuclei parallel to the ventricular surface (490 min), and the daughter cell nuclei migrate as a couple basally toward the neuronal layers (500–620 min), with one of them entering it before the end of the time-lapse (arrow, 620 min).

first 4–6 h after mitosis (Fig. 4 *a* and *c*, apical). Fourth, the increase in GFP fluorescence in the trailing daughter cell nucleus was followed by an increase in the apparent nuclear size as compared to the leading daughter cell nucleus (Fig. 4*d*, left columns).

We conclude that the apical divisions of *Tis21*-GFP-expressing NE cells in the telencephalon are asymmetric. One daughter cell becomes a neuron, leaves the VZ, and loses its GFP fluorescence. The other daughter cell remains a neuron-generating NE cell, stays in the VZ, reinduces *Tis21*-GFP expression, undergoes interkinetic nuclear migration, and divides again at the apical surface.

Basal Neuron-Generating Progenitors Undergo Symmetric Division.

Unlike daughter cells from apical divisions, the daughter cells from basal divisions behaved similarly to each other. First, in essentially all cases tracked for a sufficiently long time (Fig. 3 *c* and *d*, and Movies 2 and 3, which are published as supporting information on the PNAS web site), the sister cells shared the same destination. Both daughter cells, as judged from their GFP-labeled nuclei, migrated basally, left the VZ and entered the adjacent layer containing young neurons (Fig. 3 *c* 400–510 and *d* 500–620 min). Second, the basally directed migration of the daughter cell nuclei appeared to occur with similar speed

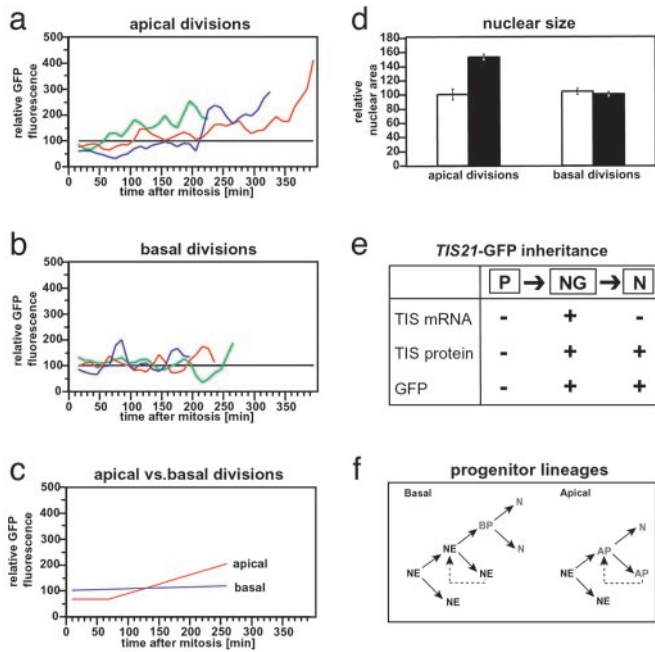


Fig. 4. Apical vs. basal neuronal progenitors and their lineages: analysis of *Tis21*-driven GFP expression and nuclear size of daughter cells. (a–c) Time course of GFP fluorescence. Total GFP fluorescence was determined in the daughter cells originating from divisions at the apical surface (a) and in the basal region (b) of the VZ. For each of the time points (10-min intervals), the total GFP fluorescence in the daughter cell with a lesser integral of total GFP fluorescence over time was set to 100 (black lines), and the total GFP fluorescence in the other daughter cell was expressed relative to this (colored curves). (a and b) The curves show the moving average of two consecutive time points each. The curves showing a consistent increase in relative GFP fluorescence (a) correspond, in each case, to the trailing daughter cell that remained in a were used to calculate the mean values for (i) the initial GFP fluorescence, (ii) the lag phase before the GFP fluorescence increase, and (iii) the GFP fluorescence increase over time by using linear regression analysis (red line). Similarly, the relative GFP fluorescence data of the three curves shown in b, which did not show a consistent increase, were used to calculate the mean value for the GFP fluorescence over time by using linear regression analysis (blue line). (d) Increase in the size of the nucleus. The area of the GFP-stained nucleus over time was determined in the daughter cells originating from divisions at the apical surface (left columns) and in the basal region of the VZ (right columns). In two of three cases of apical divisions, the area of the nucleus of one of the daughter cells increased, relative to that of the other daughter cell, during the length of the time-lapse observation (left open column, relative area initially after mitosis; left filled column, relative area at the end of the time-lapse). Note that, in each case, this increase in nuclear size occurred in the daughter cell that also showed an increase in relative GFP fluorescence, migrated more slowly in the basal direction, and remained in the VZ. No such size increase was observed for the daughter cells originating from basal divisions (right columns). Data are the mean of two (left) and three (right) observations; bars indicate the variation of the individual values from the mean and the SD, respectively. (e) Scheme summarizing the expression of the *Tis21* gene in neuronal progenitors and the passive inheritance of the TIS21 protein (22) and GFP (this study) by newborn neurons. P, NE cells undergoing proliferative division; NG, neuronal progenitors undergoing neuron-generating division; N, newborn neuron; arrows indicate lineage relationship. (f) Putative lineages of basal versus apical *Tis21*-GFP-expressing neuronal progenitors (green). NE, NE cell; AP, apical progenitor; BP, basal progenitor; N, neuron. Dashed lines indicate multiple rounds of asymmetric division.

(Table 2). Third and fourth, there was no significant difference between the daughter cells with regard to the intensity of GFP fluorescence over time (Fig. 4b and c, basal) and their apparent nuclear size (Fig. 4d, right columns). We conclude that the divisions of *Tis21*-GFP-expressing progenitors in the basal region of the VZ of the telencephalon (see also Fig. 7e and f) are

symmetric, with both daughters leaving the VZ and becoming neurons.

Discussion

We have taken a comprehensive approach to analyze the generation of neurons in the mammalian CNS. By specifically labeling the vast majority, if not all, of the neuron-generating progenitors within the neural tube in *Tis21*-GFP knock-in mouse embryos, we found that, at the onset of neurogenesis, neurons are generated by two distinct types of divisions: (i) apical asymmetric divisions of NE cells, which give rise to one neuron and one NE cell that apparently undergoes another neuron-generating division, and (ii) symmetric divisions of progenitors at the basal side of the VZ, which give rise to two neurons (Fig. 4f).

Two lines of evidence indicate that, in the *Tis21*-GFP knock-in mouse embryos, we specifically labeled most, if not all, neuron-generating progenitors in the neural tube. The first line of evidence concerns the use of the *Tis21* gene to drive GFP expression (Fig. 4e). GFP fluorescence was found to appear throughout the neural tube in exact correlation with the temporal and spatial gradients of neurogenesis, consistent with the findings that the *Tis21* mRNA is specifically expressed in neuron-generating, but not proliferating, NE cells irrespective of any regional patterning (22, 24). The onset of GFP expression was confined to the mitotically active layers, i.e., the VZ and, once present, in addition the SVZ, where fluorescence became detectable in an increasing proportion of cells as more and more neurons were generated during development. GFP fluorescence was also observed in newborn neurons, in which it appeared to decrease with their age. This is in agreement with the previous findings that the *Tis21* gene is solely transcribed in neuronal progenitors but not in neurons (22, 24), and with the notion that GFP synthesized in neuronal progenitors will be passively inherited by their daughter cells, i.e., the neurons (Fig. 4e). The observation that virtually all newborn neurons are GFP-positive (Table 1) therefore implies that most, if not all, neurons must be derived from GFP-expressing progenitors, i.e., the vast majority of neuronal progenitors transcribe the *Tis21* gene and hence produce GFP. In other words, *Tis21* expression is a “pan-neurogenic” marker.

The second line of evidence concerns how the progeny of GFP-expressing progenitors behave. Whenever the daughter cells of GFP-positive progenitors could be observed for a sufficiently long time, one or both of them left the VZ. Given that the only other cell type produced by NE cells at this early stage of CNS development are neurons (20, 29, 30), which characteristically leave the VZ, it follows that most, if not all, of the GFP-labeled progenitors are neuron-generating. The present approach of exploiting the pan-neurogenic nature of *Tis21* gene expression to reveal, specifically and throughout the neural tube, neuron-generating cell divisions explains why a population of basal neuronal progenitors in addition to the canonical apically dividing NE cells was uncovered.

Analysis of the progeny of neuron-generating divisions of NE cells at the apical surface of the VZ (see *Supporting Text* for relationship to radial glial cells) revealed that, at the onset of neurogenesis, these divisions are asymmetric with regard to daughter cell fate (Fig. 4f and Fig. 10d, which is published as supporting information on the PNAS web site). The present demonstration that, at the onset of neurogenesis, the neuron-generating divisions of NE cells at the apical side of the VZ are asymmetric is fully in line with the results of previous studies performed at later stages of neurogenesis (8, 9) and supports the canonical view that neurons arise from asymmetric divisions of NE/radial glial cells at the apical side of the VZ.

In the light of this, the finding of neuron-generating progenitors dividing in the basal part of the VZ (rather than at its apical surface) was unexpected. In contrast to the mitotic NE cells at the apical side of the VZ, of which only a minor fraction (<20%) expressed GFP, i.e., turned into neuron-generating progenitors,

nearly all (90%) of the basal mitotic cells were GFP-positive, and a small fraction (<10%) already expressed the neuronal marker β III-tubulin. The basally dividing neuron-generating progenitors occurred primarily in the neocortex and coexisted with apically dividing neuron-generating NE cells from the onset of neurogenesis. Time-lapse analysis revealed that in contrast to the asymmetric neuron-generating divisions at the apical side of the VZ, both daughter cells originating from basal neuron-generating divisions migrated out of the VZ and did not show a differential increase in nuclear volume or reinduction of GFP in one of the daughters, consistent with both of them becoming neurons. Hence, in mammals there exists, in particular in the neocortex and from the onset of neurogenesis, a second, hitherto uncharacterized, type of neuronal progenitor, which generates neurons by symmetric divisions at the basal side of the VZ (Figs. 4f and 10c).

These results contribute to resolving the issue as to the origin of CNS neurons. Retroviral lineage studies (5, 15, 16, 18) and clonal analysis of isolated neuronal progenitors (19–21) have shown that neurons can be generated from both symmetric and asymmetric divisions. However, only asymmetric divisions have previously been reported from time-lapse analyses of neuron-generating divisions of NE/radial glial cells occurring at the apical side of the VZ (7–9). The present description of a second, symmetrically dividing, type of neuronal progenitor in the basal part of the VZ reconciles those seemingly inconsistent previous reports with each other.

Mitotic cells in the basal part of the VZ have been noticed previously, but their role has been unclear. On the one hand, the observed increase in nonapical mitotic cells concomitant with the progression of neurogenesis has led to the suggestion that these cells could contribute to neurogenesis (31, 32). On the other hand, basal mitotic cells may be the progenitors of the SVZ, which constitutes a distinct cell layer at later stages of neurogenesis and which is thought to largely generate glia (26, 29). However, the recent observations that dividing SVZ cells and cortical neurons both express of certain genes (33–35) and that mutants affecting SVZ development also affect the generation of upper-layer cortical neurons (34) have been interpreted in favor of a role of dividing SVZ cells also in neurogenesis. This is fully consistent with the direct evidence presented here,

showing that the majority of cortical neurons originate from basal progenitors of the VZ and, later, the SVZ.

We believe that (at least some of) the basal *Tis21*-GFP-expressing neuronal progenitors originate from apically dividing *Tis21*-GFP-negative NE cells (Fig. 4f). First, the time course of appearance of apical versus basal *Tis21*-GFP-positive progenitors was distinct, with the basal progenitors being slightly delayed compared to the apical ones. Second, at later stages of neurogenesis in the telencephalon, *Tis21*-GFP-expressing mitotic basal progenitors outnumber apical ones, and hence at least some of the basal progenitors must initiate GFP expression *de novo*. In our model, the basal progenitor (Fig. 4f) constitutes an additional mitotic cell intermediate that, like the postmitotic neuron arising from apical progenitors (Fig. 4f), originates from an asymmetric, albeit *Tis21*-GFP-negative, division.

The basal neuronal progenitor described here has significant implications for mammalian CNS development and, perhaps, evolution. With the progression of neurogenesis in the telencephalon, the basal neuronal progenitors outnumber the apical ones and constitute the predominant population of neuronal progenitors. Considering that basal progenitors will generate twice as many neurons as apical progenitors (Fig. 4f), the basal progenitors appear to be the major source of cortical neurons. Moreover, by constituting an additional mitotic zone, basal neuronal progenitors provide a means of increasing the number of neurons that can be generated per luminal surface area of neuroepithelium per unit time (Fig. 4f). In this context, it is important to note that basal neuronal progenitors predominate in the region of the neural tube where the greatest number of neurons is generated, the telencephalon. Interestingly, there has been a substantial increase in the ratio of SVZ to VZ during evolution (34, 36). This most likely reflects the ratio of basal to apical neuronal progenitors as the neocortex enlarged. Accordingly, in humans, progenitors in the SVZ have recently been implicated in neocortical neurogenesis (35).

We thank Drs. E. Fuchs and H. Monyer for support with the ES cell work, Dr. J.-P. Rouault for the *Tis21* genomic clone, P. Vegh for excellent technical assistance, and Drs. F. Calegari, V. Dubreuil, Y. Kosodo, and especially M. Meredith-Stewart for their helpful comments on the manuscript. W.B.H. was supported by Deutsche Forschungsgemeinschaft Grants SPP 1109, Hu 275/7, SPP 1111, and Hu 275/8 and the Fonds der Chemischen Industrie.

- Rakic, P. (1988) *Science* **241**, 170–176.
- McConnell, S. K. (1995) *Neuron* **15**, 761–768.
- Huttner, W. B. & Brand, M. (1997) *Curr. Opin. Neurobiol.* **7**, 29–39.
- Caviness, V. S., Takahashi, T. & Nowakowski, R. S. (2000) in *Results and Problems in Cell Differentiation*, Mouse Brain Development, eds. Goffinet, A. M. & Rakic, P. (Springer, Berlin), Vol. 30, pp. 107–143.
- Cai, L., Hayes, N. L., Takahashi, T., Caviness, V. S., Jr., & Nowakowski, R. S. (2002) *J. Neurosci. Res.* **69**, 731–744.
- Fishell, G. & Kriegstein, A. R. (2003) *Curr. Opin. Neurobiol.* **13**, 34–41.
- Chenn, A. & McConnell, S. K. (1995) *Cell* **82**, 631–641.
- Noctor, S. C., Flint, A. C., Weissman, T. A., Dammerman, R. S. & Kriegstein, A. R. (2001) *Nature* **409**, 714–720.
- Miyata, T., Kawaguchi, A., Okano, H. & Ogawa, M. (2001) *Neuron* **31**, 727–741.
- Hämmerle, B., Vera-Samper, E., Speicher, S., Arencibia, R., Martinez, S. & Tejedor, F. J. (2002) *Dev. Biol.* **246**, 259–273.
- Zhong, W. (2003) *Neuron* **37**, 11–14.
- Rakic, P. (1995) *Trends Neurosci.* **18**, 383–388.
- Kornack, D. R. (2000) *Brain Behav. Evol.* **55**, 336–344.
- Wodarz, A. & Huttner, W. B. (2003) *Mech. Dev.* **120**, 1297–1309.
- Kornack, D. R. & Rakic, P. (1995) *Neuron* **15**, 311–321.
- Mione, M. C., Cavanagh, J. F., Harris, B. & Parnavelas, J. G. (1997) *J. Neurosci.* **17**, 2018–2029.
- Reid, C. B., Tavaoizo, S. F. & Walsh, C. A. (1997) *Development (Cambridge, U.K.)* **124**, 2441–2450.
- Reznikov, K., Acklin, S. E. & van der Kooy, D. (1997) *Dev. Dyn.* **210**, 328–343.
- Qian, X., Goderie, S. K., Shen, Q., Stern, J. H. & Temple, S. (1998) *Development (Cambridge, U.K.)* **125**, 3143–3152.
- Qian, X., Shen, Q., Goderie, S. K., He, W., Capela, A., Davis, A. A. & Temple, S. (2000) *Neuron* **28**, 69–80.
- Shen, Q., Zhong, W., Jan, Y. N. & Temple, S. (2002) *Development (Cambridge, U.K.)* **129**, 4843–4853.
- Iacopetti, P., Michelini, M., Stuckmann, I., Oback, B., Aaku-Saraste, E. & Huttner, W. B. (1999) *Proc. Natl. Acad. Sci. USA* **96**, 4639–4644.
- Haydar, T. F., Bambrick, L. L., Krueger, B. K. & Rakic, P. (1999) *Brain Res. Prot.* **4**, 425–437.
- Iacopetti, P., Barsacchi, G., Tirone, F., Maffei, L. & Cremsi, F. (1994) *Mech. Dev.* **47**, 127–137.
- Lee, M. K., Tuttle, J. B., Rebhuhn, L. I., Cleveland, D. W. & Frankfurter, A. (1990) *Cell Motil. Cytoskel.* **17**, 118–132.
- Bayer, S. A. & Altman, J. (1991) *Neocortical Development* (Raven, New York).
- Helmchen, F. & Denk, W. (2002) *Curr. Opin. Neurobiol.* **12**, 593–601.
- Haydar, T. F., Ang, E., Jr., & Rakic, P. (2003) *Proc. Natl. Acad. Sci. USA* **100**, 2890–2895.
- Jacobson, M. (1991) *Developmental Neurobiology* (Plenum, New York).
- Parnavelas, J. G. (1999) *Exp. Neurol.* **156**, 418–429.
- Smart, I. H. M. (1973) *J. Anat.* **116**, 67–91.
- Smart, I. H. M. & McSherry, G. M. (1982) *J. Anat.* **134**, 415–442.
- Ishii, Y., Nakamura, S. & Osumi, N. (2000) *Brain Res. Dev. Brain Res.* **119**, 307–320.
- Tarabykin, V., Stoykova, A., Usman, N. & Gruss, P. (2001) *Development (Cambridge, U.K.)* **128**, 1983–1993.
- Leticic, K., Zoncu, R. & Rakic, P. (2002) *Nature* **417**, 645–649.
- Rakic, P. (2003) *Cereb. Cortex* **13**, 541–549.